Macromolecules

ARTICLE

pubs.acs.org/Macromolecules

Production of Ethylene/α-Olefin/1,9-Decadiene Copolymers with Complex Microstructures Using a Two-Stage Polymerization Process

Saeid Mehdiabadi[†] and João B. P. Soares[*,‡]

[†]Department of Chemical Engineering, Razi University, Kermanshah, Iran

[‡]Department of Chemical Engineering, University of Waterloo, Waterloo, Ontario, Canada N2L 3G2

ABSTRACT: Ethylene was copolymerized with 1,9-decadiene using methylaluminoxane-activated *rac*-Et(Ind)$_2$ZrCl$_2$ at 120 °C to produce macromonomers with pendant and terminal vinyl groups with a maximum of 6.5 vinyl groups per polymer chain. The macromonomers were copolymerized with ethylene and 1-butene or 1-octene using a constrained geometry catalyst (dimethylsilyl(*N*-*tert*-butylamido)(tetramethylcyclopentadienyl)-titanium dichloride) at 120 °C in toluene. The resulting branched polymers showed three distinct populations during crystallization analysis fractionation, indicating the formation of a new fraction produced by the incorporation of macromonomer chains into ethylene/1-butene or ethylene/1-octene copolymer chains. These novel polyolefins have complex branched structures consisting of three main components: a high-crystallinity fraction (macromonomers), a low-crystallinity (or amorphous) fraction (α-olefin copolymer), and a third component resulting from the cross-linking of the two previous components (*cross-product*). These branch−block copolymers have microstructures that can be tightly controlled by varying the conditions during the two stages of polymerization required for their synthesis and are promising new materials for specialty polyolefin applications.

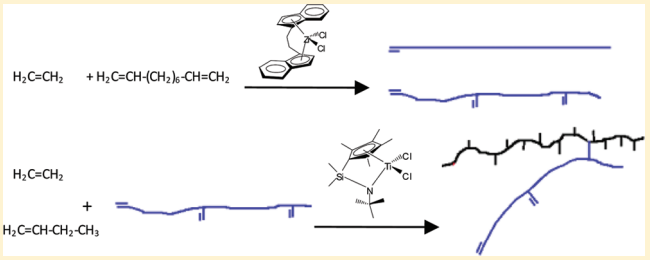

INTRODUCTION

Metallocene catalysts enable the production of polyolefins with narrow molecular weight distribution (MWD) and uniform comonomer composition distribution (CCD). Certain metallocenes, such as constrained geometry catalysts, can also form polymers with long chain branches (LCB) and good processabilities, while keeping the MWD quite narrow. The use of mixed metallocene catalysts results in more degrees of freedom to make polyethylene resins with designed microstructural properties. Dual metallocene systems have been used to produce polyolefins with bimodal MWD and CCD,[1−6] to maximize LCB formation in polyethylene,[7−9] and to produce branched and linear olefin block copolymers.[10−12]

It has been shown that by the proper selection of catalyst pairs, comonomer types, and polymerization conditions, it is possible to make copolymers with properties of thermoplastic elastomers.[12,13] Olefin copolymerization with dienes opens up the possibility of creating chains with pendant double bonds that act as macromonomers with increased likelihood of being incorporated into a growing polymer chain formed on another catalyst site.

Several articles have been published on the copolymerization of ethylene and 1,5-hexadiene with homogeneous metallocenes, showing that 1,5-hexadiene is preferentially incorporated into the polymer backbone as a five-membered ring instead of a generating pendant vinyl group.[14−18] Selectivity toward cyclization was reported to decrease when diene concentration increased over 50 mol %.[15]

Ethylene copolymerization with 1,7-octadiene using a constrained geometry catalysts (CGC) has shown that the diene molecules were inserted as cyclic structures like 1,3-cycloheptane and 1,5-cyclononane in the main polyethylene chain, with 1,5-cyclononane being the dominant ring structure.[19,20] Several bridged and nonbridged zirconocene catalysts were also investigated for copolymerization of ethylene and 1,7-octadiene at 40 °C to conclude that zironocenes with indenyl ligands produced copolymers having 1,3-disubstituted cycloheptane units, while zirconocenes with cyclopentadienyl or pentamethylcyclopentadienyl ligands gave 1-hexenyl pendant branches along the main polymer chain or 1,3-disubstituted cycloheptane units.[21] Finally, the copolymerization of ethylene and 1,9-decadiene was shown to generate 1-octenyl branches or loosely cross-linked polyethylene, depending on the type of metallocene used during the polymerization.[21]

In this article, ethylene and 1,9-decadiene were copolymerized using *rac*-Et(Ind)$_2$ZrCl$_2$ to make macromonomers with varying number of pendant vinyl groups. These macromonomers were copolymerized with ethylene and α-olefins (1-butene and 1-octene) on a separate polymerization step using dimethylsilyl-(*N*-*tert*-butylamido)(tetramethylcyclopentadienyl)titanium dichloride (CGC−Ti) to create complex polymers with branched structures composed of three main components: a high-crystallinity fraction (macromonomers), a low-crystallinity (or amorphous) fraction (α-olefin copolymer), and a third component resulting from

Received: June 20, 2011
Revised: September 1, 2011
Published: September 21, 2011

ACS Publications © 2011 American Chemical Society

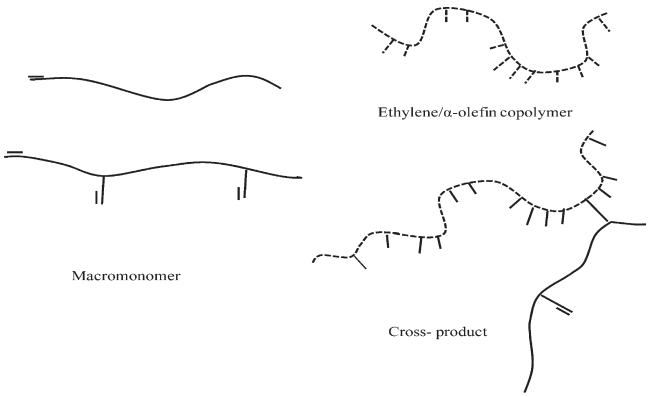

Figure 1. Microstructure classification of branch−block copolymers.

the cross-linking of the two previous components (*cross-product*). Figure 1 illustrates this classification. The whole product made after the second stage of polymerization will be referred to as *branch−block copolymer*.

EXPERIMENTAL SECTION

Materials. Methylaluminoxane (MAO, 10 wt % in toluene, Sigma-Aldrich) was used as received. Ethylene and nitrogen (Praxair) were purified by passing through molecular sieves (3 and 4-Å) and copper(II) oxide packed beds. Toluene (EMD) was purified by distillation over *n*-butyllithium/styrene/sodium and passed through two packed columns in series filled with molecular sieves (3, 4, and 5 Å) and Selexorb. All air-sensitive compounds were handled under inert atmosphere in a glovebox.

The catalysts, *rac*-ethenebis(indenyl)zirconium dichloride (*rac*-Et-$[Ind]_2ZrCl_2$) and dimethylsilyl(*N-tert*-butylamido)(tetramethylcyclopentadienyl)titanium dichloride (CGC−Ti), were purchased as powders from Sigma-Aldrich and Boulder Scientific, respectively, and were dissolved in toluene, which was first distilled over metallic sodium and then passed through a molecular sieve bed, before polymerization.

Polymer Synthesis. All polymerizations were performed in a 500 mL Parr autoclave reactor operated in semibatch mode. The polymerization temperature was controlled using an electrical band heater and internal cooling coils. The reaction medium was mixed using a pitched-blade impeller connected to a magneto-driver stirrer, rotating at 2000 rpm. Prior to use, the reactor was heated to 125 °C, evacuated, and refilled with nitrogen six times to reduce the oxygen concentration in the reactor; then, 250 mL of toluene and 0.5 g of triisobutylaluminum (TIBA) were charged to the reactor. The reactor temperature was increased to 120 °C and kept constant for 20 min for stabilization. Finally, the reactor contents were blown out under nitrogen pressure. This procedure ensures excellent removal of impurities from the reactor walls.

To make macromonomer, 200 mL of toluene was charged into the reactor, followed by 0.58 g of MAO (10 wt %), introduced via a 5 mL tube and a 20 mL sampling cylinder connected in series with an ethylene pressure differential of 50 psig. A specified volume of toluene was placed in the sampling cylinder before injection to wash the tube wall from any MAO solution. Then the band heater was powered on to commence heating of the reactor up to 120 °C. Ethylene was fed to the reactor until the solvent was saturated with ethylene and the total pressure reached 120 psig. After approximately 10 min, when the reactor temperature set point was reached and kept at a stable value, catalyst solution was injected using the same method for MAO injection, but with a lower pressure differential to ensure a minimum pressure increase in the reactor at the start of the polymerization, but still enough to transfer the catalyst solution completely to the reactor. Ethylene was supplied on demand to maintain a constant reactor pressure of 120 psig and monitored with a mass flow meter. With the exception of a short duration 1−2 °C exotherm upon catalyst injection, the temperature was kept at 120 °C ± 0.15 °C throughout all polymerizations. After 15 min, the polymerization was stopped by closing the ethylene valve and immediately blowing out the reactor contents into a 2-L beaker filled with 400 mL of ethanol. The polymer produced was then kept overnight, filtered, washed five times with ethanol, dried in air, and further dried under vacuum.

The branch−block copolymers were made separately from the macromonomers, in a sequential process.[22] After charging the reactor with a specified amount of macromonomer and removing air from the reactor by alternating vacuum and nitrogen purging cycles, solvent was added and the reactor was heated to 120 °C at high stirring rate to dissolve the macromonomer followed by the addition of cocatalyst. An appropriate amount of comonomer (1-butene or 1-octene) was then added to the reactor. Finally, the reactor was pressurized with ethylene up to the desired polymerization pressure. The reactor was equilibrated at 120 °C for 10 min. Catalyst was injected using a 5 mL catalyst injection tube connected to a 20 mL sampling cylinder filled with a specified volume of toluene to wash the tube walls from any catalyst solution and guarantee that catalyst transfer was complete. After 10−15 min of polymerization, the reactor contents were forced out of the reactor (using nitrogen pressure) into a beaker containing ethanol to stop the polymerization. Washing and drying of the polymer were performed the same way as for macromonomers.

Polymer Characterization. The polymer MWD and averages were measured at 135 °C with a Polymer Char high-temperature gel permeation chromatograph (GPC), under a trichlorobenzene (TCB) flow rate of 1 mL/min. A column bank of three PLgel Olexis 13 μm mixed pore type 300 × 7.5 mm columns were used for GPC separations. The GPC was equipped with three detectors in series (infrared, 15° angle light scattering and differential viscometer) and calibrated with polystyrene narrow standards.

The ^{13}C NMR spectrum was taken on a Bruker 500 MHz spectrometer. The probe temperature was set at 120 °C. Acquisition parameters were optimized for quantitative NMR, including a 14 micro second 90° pulse, inverse gated proton decoupling and 10 s delay time between pulses. A total of 10 000 scans were used for data averaging of homopolymers and 5000 for copolymers. The peak with highest intensity was referenced to 30.0 ppm. Deuterated *o*-dichlorobenzene was used to obtain the field-frequency lock.

Crystallization analysis fractionation (CRYSTAF) was performed using a Polymer Char CRYSTAF model 200. The polymer sample was dissolved in 47 mL of 1,2,4-trichlorobenzene at a concentration of 0.6 mg/mL. The polymer solution was heated to 160 °C and held for 2 h to ensure complete dissolution, followed by decreasing the temperature to 105 °C and stabilizing for another 55 min. A constant cooling rate of 0.1 °C/min was applied during all analyses until the temperature reached 30 °C. Polymer concentration in the solution phase was monitored using an in-line infrared detector.

Ethyl and hexyl branch distribution were determined using the in-line infrared detector coupled with GPC.[23] The Zimm−Stockmeyer approach was used to determine the degree of long chain branching. Detailed calculation procedures were described elsewhere.[23]

RESULTS AND DISCUSSION

Macromonomer Synthesis. Ethylene was copolymerized with different 1,9-decadiene concentrations using *rac*-Et-$[Ind]_2ZrCl_2$/MAO in toluene at 120 °C and a total reactor pressure of 120 psig to make macromonomers with different pendant vinyl group frequencies. Twelve polymerization runs were performed at five different 1,9-decadiene concentrations at

Table 1. Molecular Weight Measurements for Ethylene/1,9-Decadiene Copolymers

run	diene (mmol/L)	M_w	M_n	PDI	polymer mass (g)
1	0.114	52 300	25 500	2.05	4.8
2	0.077	51 900	26 100	1.99	5.6
3	0	50 500	25 000	2.02	7.7
4	0.039	50 900	25 400	2.00	6.45
5	0.114	52 700	24 800	2.13	5.26
6	0.077	50 800	25 300	2.00	5.85
7	0	51 000	25 500	2.00	7.47
8	0.152	54 100	25 500	2.13	4.8
9	0.039	50 500	25 200	2.00	6.16
10	0.114	52 900	25 900	2.04	5.65
11	0	51 400	25 800	1.99	7.5
12	0.077	51 500	25 100	2.05	6.27

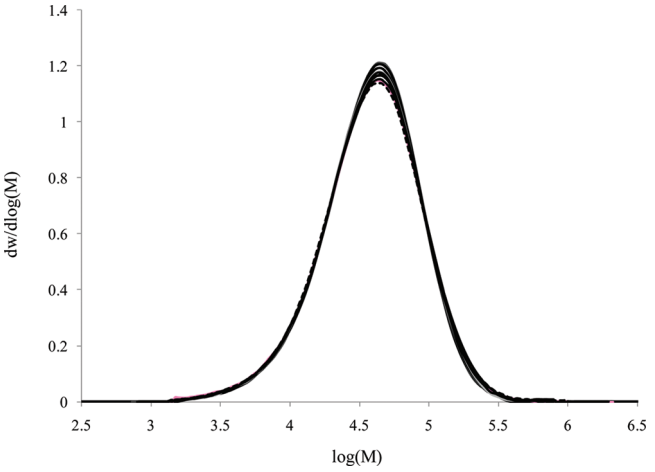

Figure 2. Molecular weight distribution of ethylene/1,9-decadiene copolymers.

Table 2. Analysis of Variance for Weight Average Molecular Weight (M_w)

source of variation	sum of squares	degrees of freedom	mean square	F_0	P value
diene concentration	12 153 500	4	3 038 400	16.06	0.0012
error	1 324 500	7	189 200		
total	13 478 000	11			

a polymerization time of 15 min. The run order was randomized to avoid biasing the experimental results. Table 1 summarizes molecular weight measurements and polymer yields for these runs.

It is hard to deduce any conclusive effect by just glancing at the weight-average molecular weights in Table 1, or even by plotting their molecular weight distributions, as shown in Figure 2. However, inferential statistics were used to show that macromonomers made with higher 1,9-decadiene concentrations also had higher weight-average molecular weights.

The molecular weight measurements shown in Table 1 can be described with the single-factor ANOVA model[24]

$$Y_{i,j} = \mu + \tau_i + \varepsilon_{i,j} \quad (1)$$

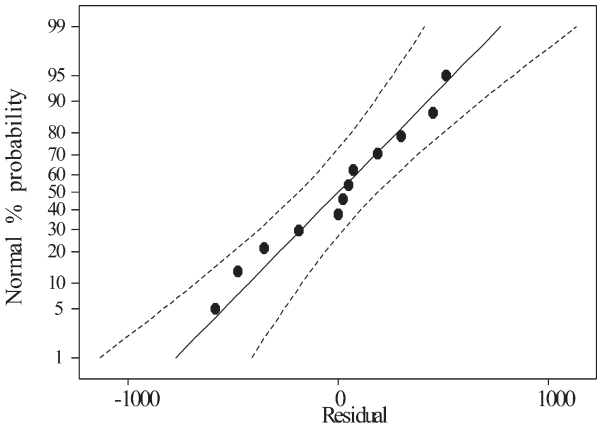

Figure 3. Normal probability plot of residuals for M_w measurements.

where $Y_{i,j}$ is the $i \times j$th measurement, μ is the overall mean, τ_i is a parameter associated with the ith treatment level (called the treatment effect—in the present case, weight-average molecular weight), and $\varepsilon_{i,j}$ is a random error component arising from all sources of variability. The null hypothesis is H_0: $\tau_1 = \tau_2 = ... = \tau_n = 0$ (where $n = 5$, different 1,9-decadiene concentrations in the reactor) and the alternative hypothesis is H_1: $\tau_i \neq 0$ for at least one value of i.

Since the number of replicates are not the same in all treatment levels (see Table 1), an unbalanced design[24] approach was used to perform the analysis of variance, as summarized in Table 2. The test statistic F_0, which is the ratio of the treatment mean square to error mean square, was used to test the null hypothesis. Because $F_0 = 16.06$ is greater than $F_{0.05\,4,\,7} = 4.12$, we reject the null hypothesis and conclude it is unlikely that the treatment means are equal. In other words, 1,9-decadiene concentration affects the molecular weight averages of the ethylene/1,9-decadiene copolymers.

The analysis of variance assumes that the measurements are normally and independently distributed with the same variance for each factor level. The normality assumption can be checked by constructing the normal probability plot of the residuals for M_w, shown in Figure 3. The error distribution seems to be normal, despite the fact that moderate departures from normality are likely to be seen with small samples. The plots of the residuals versus run order and diene concentration in the reactor also do not show any pattern, with the approximately uniform spread of residuals supporting the assumption of equal variances (these figures are not shown herein for the sake of brevity).

Figure 4 plots M_n and M_w versus decadiene concentration. A slight, but statistically significant increase in M_w is observed, which can be attributed to the higher probability of macromonomer incorporation (LCB formation reactions) onto the growing polymer chains because of the increase in pendant vinyl group frequency in the macromonomer chains. This increase is also confirmed by the intrinsic viscosity plot ($\log [\eta] \times \log M$) in Figure 5, since samples with higher diene content have a more marked deviation from linearity in the high molecular weight region.

The CRYSTAF profiles for these macromonomers are shown in Figure 6. It is clear that, as the diene content increases in the macromonomer chains, their CRYSTAF peak temperatures decrease, since the incorporation of the diene molecules generates short chain branches (SCB) that reduce the crystallizabilities of the macromonomer chains.

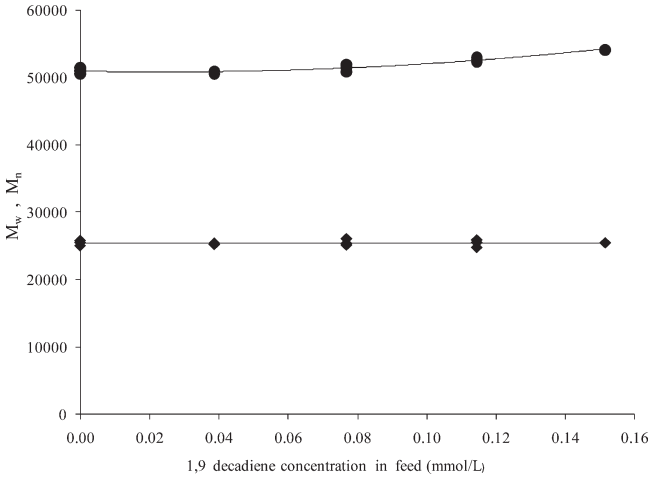

Figure 4. Number and weight-average molecular weights versus 1,9-decadiene concentration in the reactor.

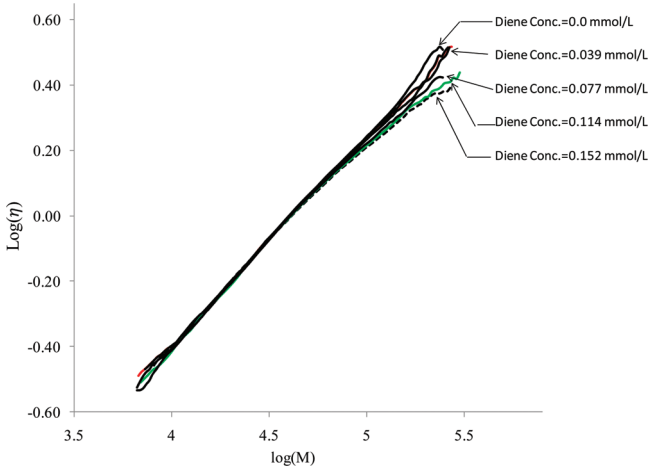

Figure 5. Intrinsic viscosity plot for ethylene/1,9-decadiene copolymers.

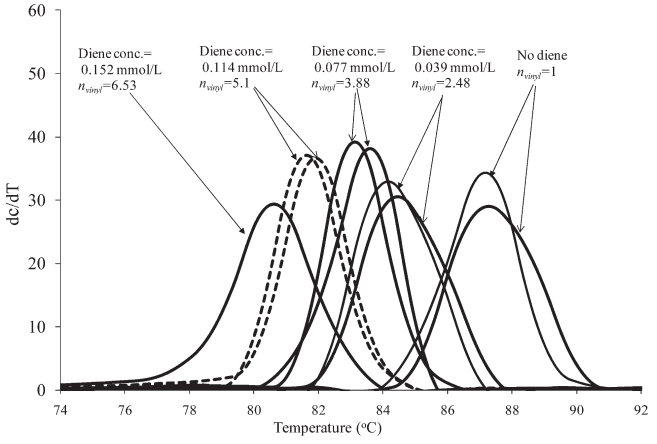

Figure 6. CRYSTAF profiles for ethylene/1,9-decadiene copolymers.

Macromonomer Structure Investigation by ^{13}C NMR. Five samples with different diene molar fractions were selected randomly for further study using nuclear magnetic resonance spectroscopy.

Figure 7 illustrates the ^{13}C NMR spectrum of an ethylene/1,9-decadiene copolymer (Run 4, Table 1). The structure shown in Scheme 1 was proposed for the ethylene/1,9-decadiene copolymers based on the peaks observed in its spectrum. The Grant and Paul rules[25,26] were used to obtain the assignments listed in Table 3.

The following equations were developed to calculate the pendant unsaturated chain end density (λ_{diene}= number of pendant vinyl groups per 10 000 carbon atoms), assuming that all pendant groups are the source of branch points in the polymer chains,

$$\lambda_{diene} = 10000 \frac{(IA_\alpha + IA_\beta + IA_{5b})}{6IA_{Tot}} \quad (2)$$

or

$$\lambda_{diene} = 10000 \frac{(IA_\alpha + IA_\beta + IA_{5b} + IA_{br})}{7IA_{Tot}} \quad (3)$$

where IA_α, IA_β, IA_{5b} and IA_{br} are the areas of the peaks for α, β, 5b, and tertiary carbon atoms, respectively. The 5b carbon atom has a lower chemical shift than the β carbon (27.22 versus 27.31), which explains the double peak at approximately 27 ppm shown in Figure 7. The deconvolution of this peak using Lorentzian functions gives an average area ratio of 1.9 for all four samples, which shows that the chemical shift assignment is correct (allowing for small deconvolution and integration errors). Therefore, $IA_\beta + IA_{5b}$ is calculated by integrating the bimodal peak from 27 to 27.5 ppm.

The number-average molecular weight was calculated using the equation below

$$\frac{1}{M_n} = \frac{\lambda_{CH_3} + \lambda_{vinyl} - \lambda_{diene}}{280000} \quad (4)$$

The unsaturated chain-end density (λ_{vinyl}, the number of unsaturated chain ends per 10 000 carbon atoms) and the saturated chain end density (λ_{CH_3}, the number of saturated chain ends per 10 000 carbon atoms) were calculated using the following equations,

$$\lambda_{vinyl} = 10000 \frac{IA_{1v}}{IA_{Tot}} \quad (5)$$

$$\lambda_{CH_3} = 10000 \frac{IA_2 + IA_3}{2IA_{Tot}} \quad (6)$$

where IA_{1v}, IA_2, IA_3, and IA_{Tot} are the integral areas of allylic, 2, 3, and total carbons, respectively. The unsaturated chain end density, λ_{vinyl}, calculated using eq 5, gives the total number of pendant and terminal vinyl groups per 10,000 carbons; the difference between λ_{vinyl} and λ_{diene} is the number of terminal vinyl bonds at the end of the polymer chains per 10,000 carbon atoms. Table 4 summarizes the results of these calculations for selected polymer samples. The last column in Table 4 also lists the number-average molecular weights measured by GPC and determined with ^{13}C NMR using eq 4, demonstrating that they are in good agreement.

Figure 8 shows how λ_{vinyl}, λ_{diene}, and λ_{CH_3} vary with the concentration of 1,9-decadiene in the reactor. Both λ_{vinyl} and λ_{diene} increase linearly with the diene concentration in the reactor, while λ_{CH_3} remains unaffected, implying that one end

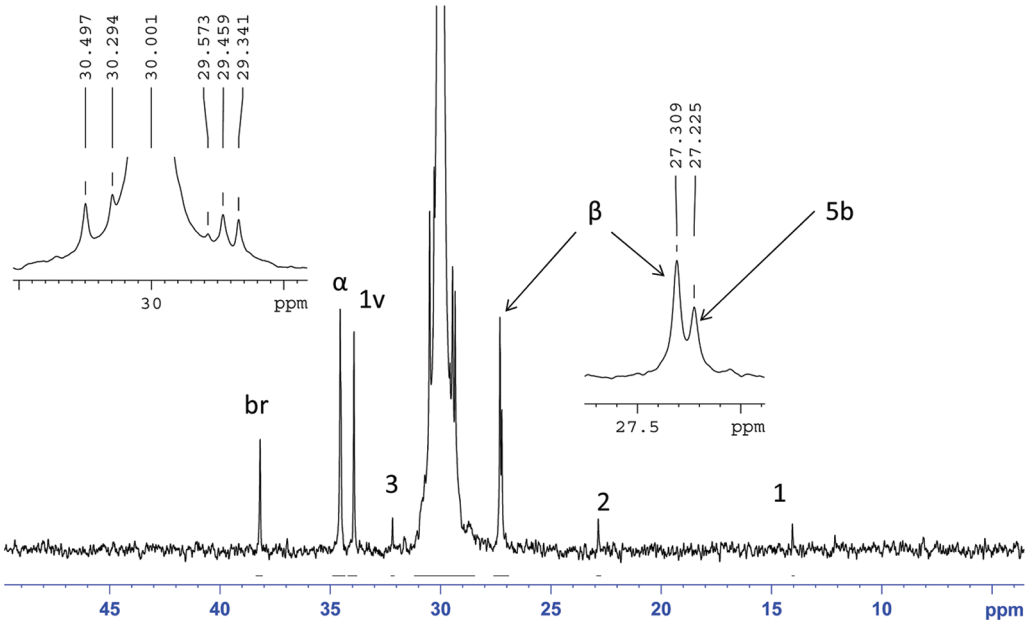

Figure 7. ^{13}C NMR spectra for poly(ethylene-*co*-1,9-decadiene) (run 4, Table 1).

Scheme 1. Carbon Nomenclature for Chemical Shift Assignments

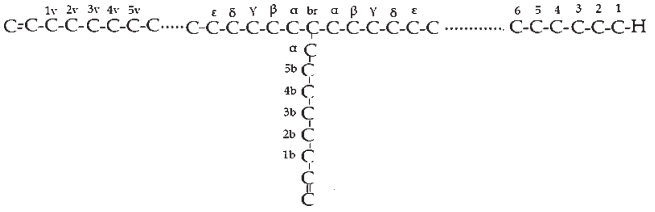

of the polymer chains is saturated and the other end has a terminal vinyl group.

Figure 8 also shows that λ_{diene} increases linearly with 1,9-decadiene concentration in the reactor. These macromonomer chains, functionalized with pendant vinyl groups, have increased possibility of being incorporated onto a growing chain made on another catalyst site (or in another reactor), leading to the formation of chains with long chain branches, as will be demonstrated below.

Three other important macromonomer microstructural characteristics are the average ethylene sequence length between diene units, n, average number of pendant unsaturated chain ends per polymer chain, n_{diene}, and average number of unsaturated chain ends per polymer chain, n_{vinyl}. Equations for calculating these properties are given below,

$$n = \frac{M_n - \frac{M_n \times \lambda_{diene} \times 111}{140,000}}{\left(\frac{M_n \times \lambda_{diene}}{140000} + 1\right) \times 28} \quad (7)$$

$$n_{diene} = \frac{\lambda_{diene} \times M_n}{140000} \quad (8)$$

$$n_{vinyl} = \frac{\lambda_{vinyl} \times M_n}{140000} \quad (9)$$

Table 3. ^{13}C NMR Chemical Shifts for Poly(ethylene-*co*-1,9-decadiene) Made with *rac*-Et-(Ind)$_2$ZrCl$_2$

	chemical shift (δ, ppm)	
resonance peak	calculated	observed
1	14.07	14.05
2	22.68	22.85
3	32.46	32.17
4	29.58	29.57
br	38	38.18
α	34.89	34.55
β	27.56	27.31
γ	30.44	30.5
δ	30.07	30
ε	30.01	30
5b	27.13	27.22
4b	30.41	30.29
3b	30.42	30.5
2b	29.58	29.57
1b	34.07	33.92
1v	34.07	33.93
2v	29.58	29.57
3v	30.3	30.3

Table 5 summarizes these calculations for the five selected samples.

Increasing the diene concentration in the reactor makes n_{diene} and n_{vinyl} increase linearly, as shown in Figure 9. Notice that $n_{vinyl} \approx 1.0$ at zero decadiene concentration, since n_{vinyl} also accounts for terminal vinyl groups in the chains. The average ethylene sequence length between the diene units, n, decreases as the decadiene concentration increases.

Figure 10 shows how CRYSTAF peak temperatures depend on n_{diene}. A linear trend is observed, indicating that the 1,9-decadiene molecules incorporated in the polyethylene chains

Table 4. ^{13}C NMR results for Poly(ethylene-*co*-1,9-decadiene) Macromonomers

run	diene (mmol/L)	λ_{vinyl}	λ_{CH_3}	λ_{diene} [a]	λ_{diene} [b]	M_n [c]	M_n [d]
3	0	5.95	5.99	0.00	0.00	23 464	25 020
4	0.039	14.69	5.34	8.18	7.56	23 625	25 400
6	0.077	22.76	4.73	15.75	15.37	23 834	25 346
5	0.114	29.84	6.12	24.40	24.11	24 224	24 759
8	0.152	37.92	5.94	32.24	31.37	24 089	25 460

[a] λ_{diene} calculated using eq 2. [b] λ_{diene} calculated using eq 3. [c] Determined using ^{13}C NMR, eq 4. [d] Measured by GPC.

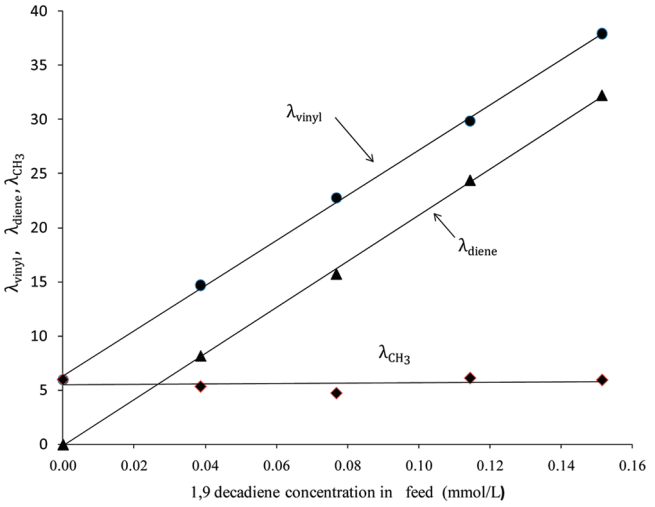

Figure 8. Dependency of λ_{vinyl}, λ_{diene}, and λ_{CH_3} with 1,9-decadiene concentration in the reactor.

Table 5. Microstructural Properties of Ethylene/1,9-Decadiene Copolymers

run	diene (mmol/L)	n	n_{diene}	n_{vinyl}
3	0	838	0	0.997
4	0.039	352	1.38	2.479
6	0.077	228	2.68	3.876
5	0.114	162	4.22	5.103
8	0.152	128	5.55	6.525

decrease their crystallizabilities, as would also be also observed for ethylene/α-olefin copolymers.

Synthesis of Branch−Block Copolymers. Two procedures may be used for the production of branch−block copolymers: simultaneous or sequential synthesis. In the simultaneous synthesis, two catalysts are added to the reactor to produce macromonomers and branch−block copolymers at the same time, while in the sequential synthesis approach, macromonomers are produced separately and then introduced in another reactor to be copolymerized with ethylene and α-olefins with a catalyst capable of incorporating macromonomers into the growing copolymer chains. In this investigation, we adopted the sequential approach because it leads to higher macromonomer incorporation, as shown in our previous simulation studies.[11,22] The procedure for making the macromonomers containing terminal and pendant vinyl groups was explained in the previous section.

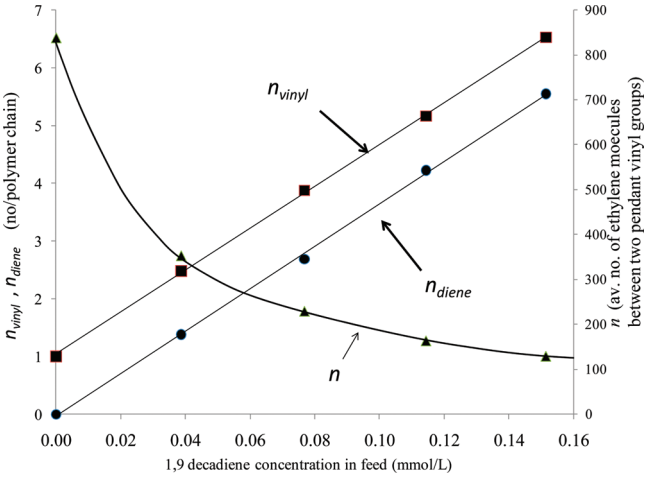

Figure 9. Average pendant unsaturated chain ends (n_{diene}), average unsaturated chain ends (n_{vinyl}) per chain and average ethylene sequence length between diene units (n) variations with 1,9-decadiene concentration in the reactor.

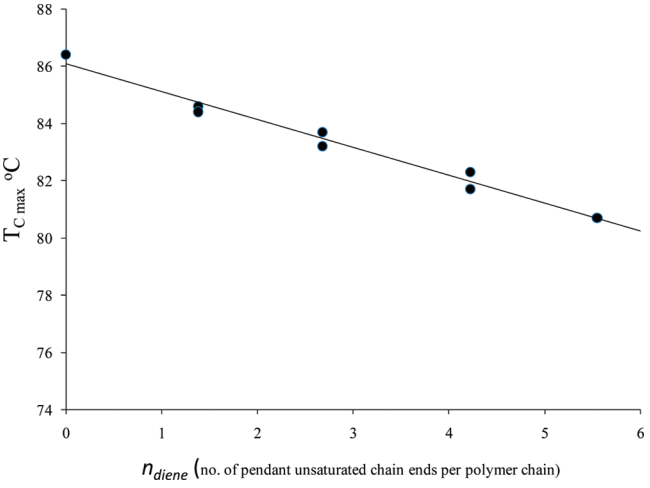

Figure 10. CRYSTAF peak temperature versus average pendant vinyl groups per chain end in copolymer.

The α-olefin comonomers used were 1-butene and 1-octene. Reaction variables tested included polymerization time, ethylene pressure, and catalyst concentration. The catalyst used for macromonomer incorporation was CGC−Ti.

Branch-Block Copolymers Made with 1-Butene. *Effect of Degree of Unsaturation of the Macromonomer.* Three polymerizations were performed with macromonomers having different vinyl group densities to produce branch−block copolymers. The CRYSTAF profiles of theses macromonomers are shown in Figure 6. Table 6 summarizes the polymerization conditions for these runs.

Molecular weights and short chain branch frequencies for the polymers made with macromonomers A, B, and C are summarized in Table 7.

Figure 11 shows the CRYSTAF profile for samples A, B, and C. Samples B and C, made with macromonomers having higher vinyl group density, are trimodal, while sample A is bimodal. The high crystallization temperature peak corresponds to unreacted macromonomer, while the low crystallinity (or soluble) peak is

Table 6. Ethylene/1-Butene Polymerization Conditions[a]

			polymer mass (g)	
sample	λ_{vinyl}(MM)[b]	n_{vinyl}(MM)[b]	total[c]	excluding macromonomer
A	5.95	1	10.9	7.9
B	22.76	3.88	15.07	12.07
C	37.92	6.53	9.36	6.36

[a] Polymerization conditions: T = 120 °C, P = 120 psig, toluene volume = 222.8 mL, 1-butene concentration = 0.63 mol/L, macromonomer concentration = 13.5 g/L, and polymerization time = 15 min. [b] MM = macromonomer. [c] Total polymer mass = macromonomer mass + mass of polymer formed in stage 2.

Table 7. Molecular Weight Measurements Using GPC and Long Chain Branch Estimates Using the Zimm−Stockmayer Equation

sample	M_w	M_n	PDI	λ_{ethyl}[a]	n_{LCB}[b]	λ_{LCBD}[c]
A	50 400	21 000	2.4	34	0	0
B	108 400	27 300	3.9	37	0.2	1.03
C	115 800	27 800	4.2	36	0.74	3.73

[a] λ_{ethyl} = average number of ethyl branches per 1,000 carbon atoms. [b] n_{LCB} = average number of LCBs per polymer chain. [c] λ_{LCB} = number of LCBs per 10,000 carbon atoms.

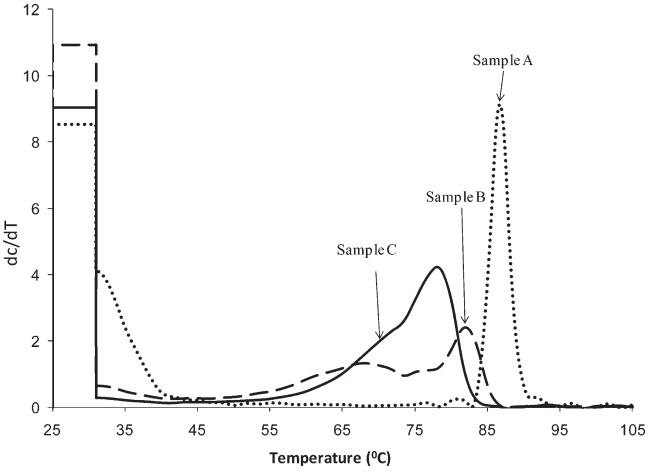

Figure 11. CRYSTAF profiles for samples A, B, and C.

formed by ethylene/1-butene low crystallinity (or amorphous) copolymer. The intermediate peak observed in samples B and C results from the incorporation of macromonomers into growing copolymer chains (cross-product). For sample C, the intermediate CRYSTAF peak and the macromonomer peak superimpose because the macromonomer has lower crystallizability due to its higher 1,9-decadiene incorporation, as illustrated in Figure 6.

Figure 12 depicts log $[\eta]$ × log M plots overlaid on the MWDs for samples A, B and C. Because of polymer coil contraction resulting from ethyl short chain branches (SCB) formed by 1-butene copolymerization, the intrinsic viscosity of sample A is lower than that for the NBS 1475 standard with no SCBs, but it follows the linear trend characteristic of polymers without LCBs. This measurement confirms our observation in Figure 11 that no cross-product was formed in sample A, which is simply a blend of

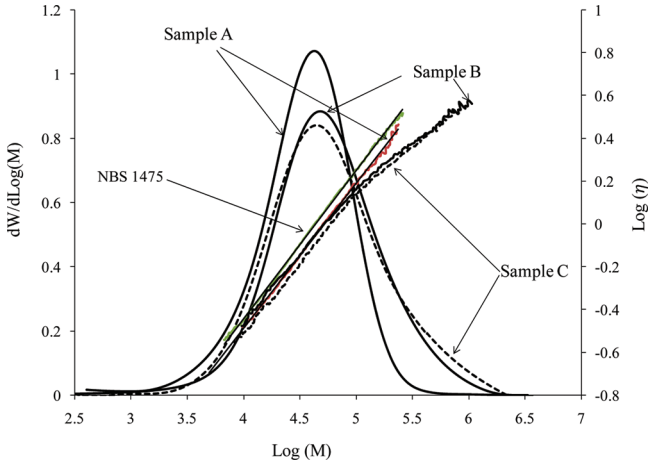

Figure 12. MWD and intrinsic viscosity plot for samples A, B, and C.

Table 8. Polymerization Conditions and Summary Results for Runs D through F[a]

			polymer mass (g)		
sample	time (min)	MM[b] (g/L)	total	excluding MM[b]	CGC−Ti (μmol/L)
D	7	13.5	13.3	10.3	8.98
E	15	13.5	6.84	3.86	6.7
F	15	0	6.5	6.5	1.8
G	15	13.5	18.6	15.6	8.98

[a] Polymerization conditions: T = 120 °C, P = 120 psig, toluene volume = 222.8 mL, and 1-butene = 0.4 mol/L. λ_{vinyl} (MM) = 22.8 vinyl groups/10 000 C atoms. [b] MM = macromonomer.

two linear polymers. The log $[\eta]$ × log MW plots for samples B and C, on the other hand, show a clear departure from linearity at higher molecular weights, indicating that those samples contain LCBs. This supports our conclusion that the intermediate CRYSTAF peak is formed by macromonomer molecules grafted onto ethylene/1-butene copolymer chains.

The average number of LCBs per polymer chain, n_{LCB}, and long chain branch density, λ_{LCB}, number of long chain branches per 10 000 C, for samples A, B, and C were also calculated using Zimm−Stockmayer equations[23] and are summarized in Table 7. The number of ethyl branches per 1,000 carbon atoms, λ_{ethyl}, are nearly the same for samples A, B, and C, as expected, since the copolymerizations were performed at the same 1-butene/ethylene ratio. It is also clear that macromonomers with higher λ_{vinyl} (see Table 6) make branch−block copolymers with higher LCB frequencies.

Finally, branch−block copolymers made with macromonomers having higher diene density have broader MWDs caused by LCB formation reactions resulting in the production of cross-product chains of higher molecular weight.

Effect of Polymerization Time and Catalyst Concentration. Four polymerization runs were performed to investigate the effect of polymerization time and catalyst concentration on cross-product formation. The polymerization conditions are summarized in Table 8.

The polymerization procedure was the same used in the previous runs. The λ_{vinyl} of the macromonomer used in the

Table 9. GPC−IR Results for Samples D to G and Macromonomer

sample	M_w	M_n	PDI	λ_{ethyl}	n_{LCB}[a]
D	187 300	41 300	4.5	25	0.62
E	73 300	25 300	2.9	19	0.16
F	96 000	38 200	2.5	29	0
G	273 300	42 100	6.5	26.3	1.03
MM	54 100	26 000	2.1	0	0.083

[a] Calculated using the Zimm−Stockmayer equation.

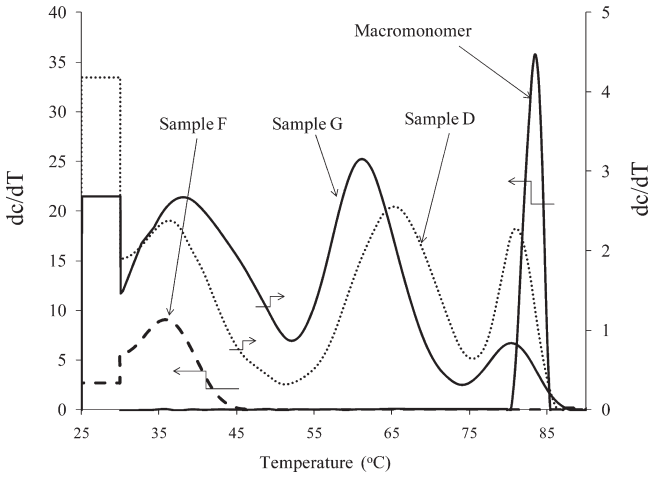

Figure 13. CRYSTAF profiles for samples D, F, G, and macromonomer.

copolymerization was 22.8 per 10 000 carbons. Run F in Table 8 is just an ethylene/1-butene copolymerization under the same conditions to locate the CRYSTAF peak for the ethylene/1-butene copolymer alone.

Runs D and G were performed to investigate the effect of polymerization time on cross-product formation. Their polymerization conditions were the same, except for polymerization time, which was 7 min for run D and 15 min for run G. Similarly, runs E and G were performed under the same polymerization conditions, except that in run E the amount of CGC−Ti injected in the polymerization reactor was lower than in run G. Table 9 summarizes molecular weight results for these polymers.

Figure 13 overlays the CRYSTAF profiles of polymers D, F, G, and macromonomer. As discussed above, if no cross-product is formed during polymerization, two CRYSTAF peaks are expected: one high-temperature peak for the macromonomer, and another low-temperature peak for the ethylene/1-butene copolymer (equivalent to that of polymer F). An intermediate third peak was observed for the samples D and G, which indicates the formation of cross-product chains through incorporation of macromonomers into low crystallinity ethylene/1-butene copolymer backbones.

The MWDs for these samples (Figure 14) also confirm the presence of branched cross-products because of the observed broadening of the MWD. Increasing polymerization time leads to an increase in molecular weight averages and long chain branch frequency of the whole polymer, as shown in Table 9. The ethylene branch density, λ_{ethyl}, of the whole polymer also increases because the mass fraction of the cross-product increases (Table 9).

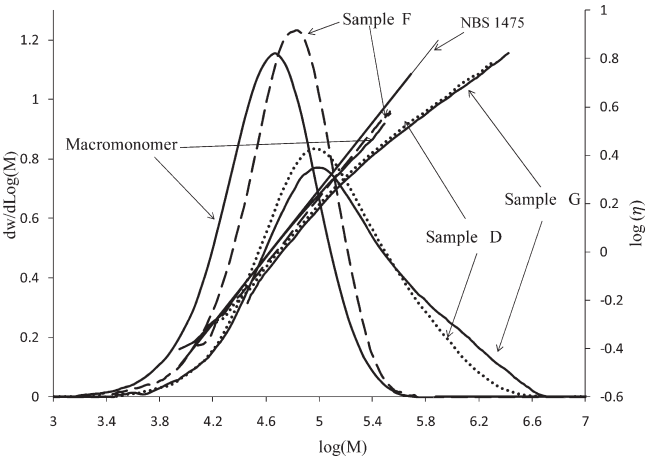

Figure 14. MWDs and Mark−Houwink plot for samples D, F, G, macromonomer, and a linear polyethylene standard (NBS 1475).

Figure 14 also shows the log $[\eta]$ × log MW plots for polymers D, F, G, macromonomer and linear NBS standard 1475. Sample F exhibits simple power law behavior described by the Mark−Houwink equation, which is indicative of linear polymers, while the curvatures of the corresponding curves for samples D and G imply the presence of LCBs. The actual structure of these LCBs is likely to be of two polymer chains connected through a bridge six carbons long, resulting from the polymerization of the pendant double bond of 1,9-decadiene units. The "main" chain is an amorphous ethylene/1-butene chain with high 1-butene content (about 30 ethyl branches per 1000 carbon atoms), while the macromonomer branch is more crystalline, with about three SCBs per polymer chain.

Long chain branch frequencies (λ_{LCB}) for the polymer samples were also calculated and are shown in Table 9. Although these numbers are not absolute, they are useful to compare the extent of LCB formation in the samples. The results in Table 9 show that increasing polymerization time leads to higher LCBF values for the whole polymer.

Samples E and G were made with different CGC−Ti concentrations and same polymerization time. Figure 15 shows the effect of changing CGC−Ti concentration on the MWD and intrinsic viscosity of the resulting copolymer. Increasing CGC−Ti concentration leads to more macromonomer incorporation (for the same polymerization time), which in turn broadens the MWD with the formation of higher molecular weight polymer. In Run E, despite the lower CGC−Ti concentration, LCBs are still formed as shown by the deviation from linearity in the log $[\eta]$ × log MW plot in Figure 15, but not enough to produce a noticeable CRYSTAF peak, only a slight shoulder (Figure 16). Run G, on the other hand, due to higher catalyst concentration which leads to more long chain branch formation, produces a noticeable intermediate CRYSTAF peak.

Ethylene Pressure Effect. The effect of ethylene pressure on the microstructural properties of the resulting terpolymers was investigated at three different ethylene partial pressures during polymerization. The λ_{vinyl} of the macromonomer used was approximately 22.8 (2.68 pendant vinyl groups per chain). CGC−Ti and cocatalyst loadings were the same for all three runs. Polymerization temperature and time were also the same, except for the highest ethylene pressure run, for which the polymerization time had to be decreased to approximately

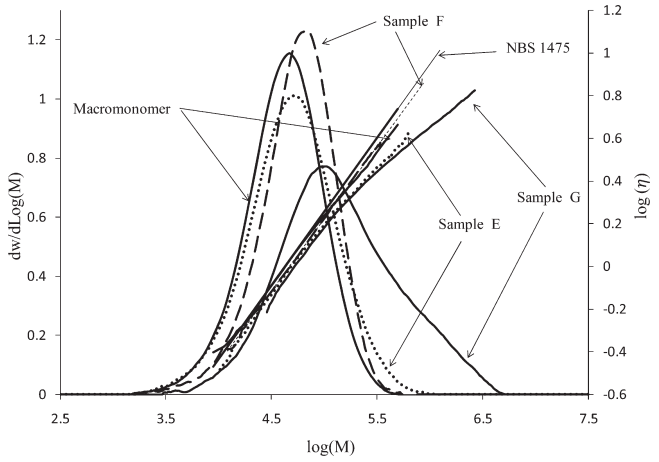

Figure 15. MWDs and Mark Howink plots for samples E, G, F, and macromonomer and a linear polyethylene standard (NBS 1475).

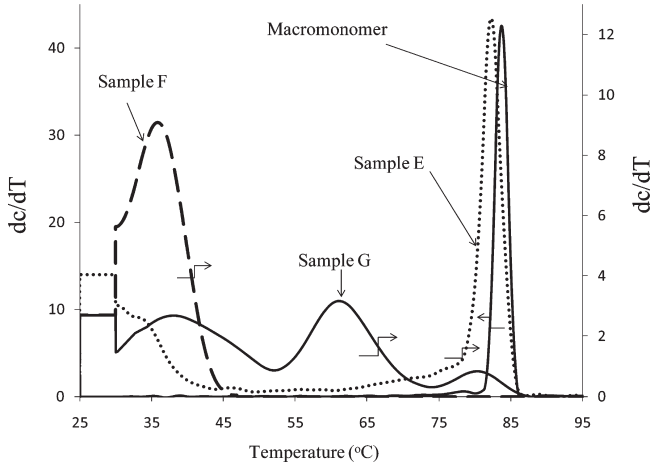

Figure 16. CRYSTAF profiles for samples E, F, G, and macromonomer.

Table 10. Polymerization Conditions for Samples H, I, and J[a]

		polymer mass (g)		
sample	total pressure (psig)	total	excluding MM	time (min)
H	46	4.6	1.6	15
I	120	11.76	8.76	15
J	200	14.04	11.04	2.8

[a] Polymerization conditions: T = 120 °C, toluene volume = 222.8 mL, 1-butene concentration = 0.63 mol/L, λ_{vinyl} (MM) = 22.8, and CGC−Ti concentration = 12.25 μmol/L.

3 min to reduce the polymer mass to an acceptable range and avoid mass and heat transfer limitations (polymer yield is directly proportional to ethylene pressure). The polymerization conditions are summarized in Table 10. Average molecular weights and SCB frequencies are shown in Table 11.

The overlay of the CRYSTAF profiles for samples H, I, and J is shown in Figure 17. Sample H, made at the lowest ethylene pressure, does not show an intermediate peak. For sample I, the left side shoulder of the macromonomer peak is attributed to

Table 11. Average Molecular Masses, SCBD, and Long Chain Branch Frequency for Samples H, I, and J

run	M_w	M_n	PDI	λ_{ethyl} whole polymer	λ_{ethyl} polymer formed by adding CGC−Ti	n_{LCB}
H	58 900	14 300	4.1	40.5	117	0.054
I	84 400	22 600	3.7	35.5	48	0.17
J	119 100	37 100	3.2	18.5	23.5	0.16
MM	54 100	26 000	2.08	0.0	-	0.081

macromonomer incorporation into the copolymer chains by the CGC−Ti catalyst. The intermediate peak for the sample J is formed by a similar mechanism. It may seem counterintuitive that increasing ethylene pressure would favor macromonomer incorporation, but this behavior seems to be related to the 1-butene fraction in the chains made by the CGC−Ti catalyst. As the ethylene pressure in the reactor increases for the same 1-butene concentration, the fraction of 1-butene in the copolymer decreases, as clearly seen in the CRYSTAF profiles depicted in Figure 17 (the copolymer peak move to higher crystallization temperatures). Because of steric effects, it is more likely that a macromonomer chain will be inserted into the growing chain terminated in an ethylene, rather than a butene, unit. Therefore, increasing the ethylene pressure at the same 1-butene concentration will indirectly favor macromonomer insertion, as illustrated in Figure 17.

Figure 18 shows the SCB distribution across the MWD for sample H, which was made at the lowest ethylene pressure. A bimodal MWD peak is observed and since the high molecular weight peak for that sample coincides with the macromonomer peak (dashed curve in Figure 18), it seems that the high molecular weight peak results from the unreacted macromonomer. This conclusion is also supported by SCB/1000 C versus molecular weight plot shown in Figure 18 because the SCB/1000 C for high molecular weight polymer chains is very low, practically in the experimental range of SCB/1000 C measured for the macromonomer alone.

Figure 18 also depicts the log $[\eta]$ × log MW plot across the MWD for sample H and macromonomer. The log $[\eta]$ × log MW plot deviates from linearity at both low and high molecular weight ends of the distribution. The deviation at the low molecular weight may be attributed to the presence of chains with higher SCB frequencies. Since the difference between the log $[\eta]$ × log MW plots for macromonomer and sample H is small, the LCB in sample H is not high, as already noticed by inspection of its CRYSTAF profile. Therefore, the small deviation at the high molecular weight region may be attributed to the presence of LCBs in the unreacted macromonomer itself. As proposed above, the high short chain branch frequency (117 SCB/1000 for lower molecular weight region) of the polymer backbone growing on CGC−Ti in sample H might cause steric hindrances which decrease the rate of macromonomer incorporation.

Figure 19 shows results for sample I, made at total pressure of 120 psi, clearly indicating the presence of LCBs, since log $[\eta]$ × log MW plot deviates from linearity significantly. Comparing the SCB distribution of sample I with the one made at the lowest pressure (Figure 18) shows a gradual, not sudden, decrease in SCB. This happens because the molecular weight of the copolymer made at higher ethylene pressure increases, making the MWD unimodal and "merging" the MWD distributions for each component in the polymer.

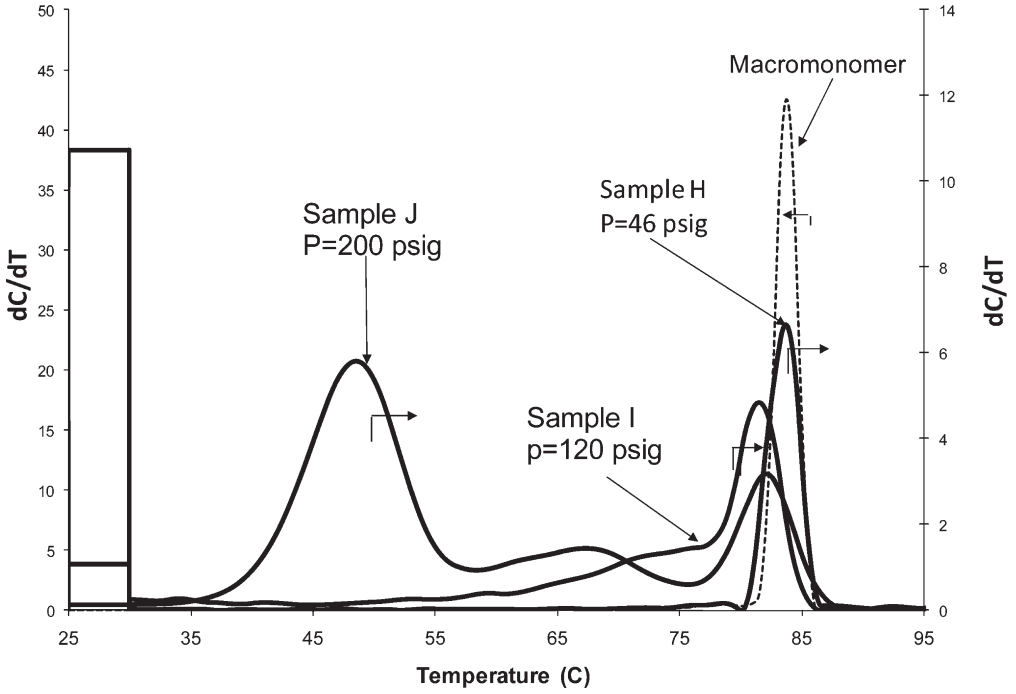

Figure 17. CRYSTAF profiles for samples H, I, J, and macromonomer.

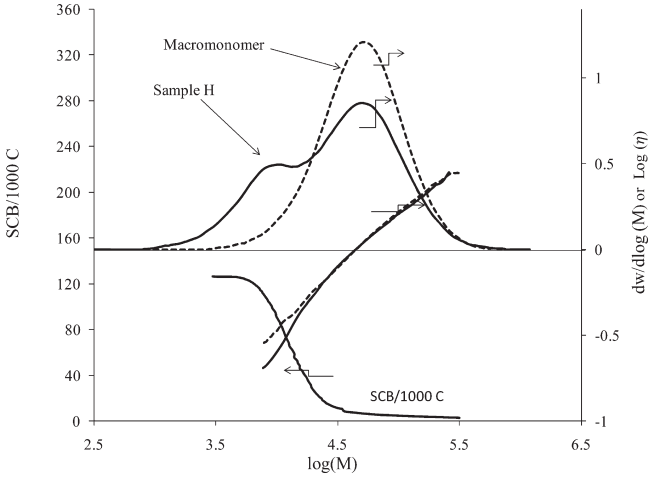

Figure 18. MWD, SCB distribution and intrintsic viscosity plot for sample H and macromonomer.

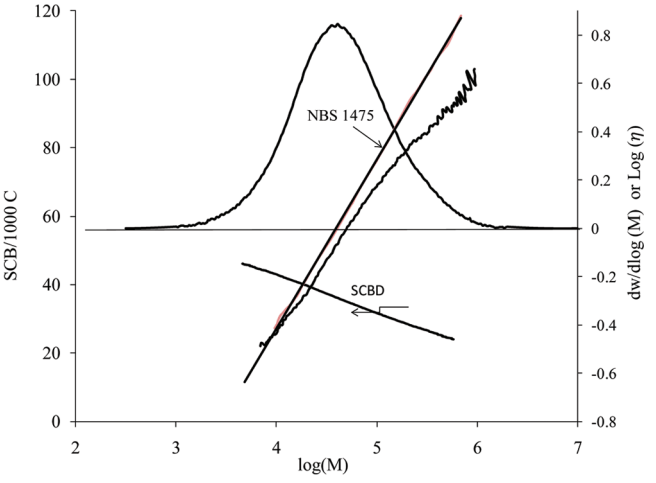

Figure 19. MWD, intrinsic viscosity plot and SCB distribution for sample I.

Figure 20 shows the log $[\eta] \times$ log MW plot for sample J. The LCB frequency of sample J is similar to that of sample I (Table 11). We can speculate that a low ethylene pressure favors the formation of LCBs, but at the same time, the higher SCB frequency in ethylene/1-butene copolymers made at lower ethylene pressures makes it harder for macromonomers to be incorporated onto these chains; these two factors, acting in opposing directions, cause the LCBF of the samples I and J, 120 and 200 psi, to be the approximately the same.

The SCB distribution as a function of molecular weight for sample J, as shown in Figure 20, is very interesting because it initially increases with molecular weight, reaches a maximum, and then decreases. This apparently abnormal behavior is easy to explain: the copolymer made at higher ethylene pressure has higher molecular weight averages than those of the macromonomer, consequently, the low MW region is mostly composed of macromonomer with low SCB content; the intermediate MW region is mostly formed by ethylene/1-butene copolymer with high SCB frequency; finally, the high MW region contains most of the cross-product, which is formed by copolymer (high SCB) and macromonomer (low SCB) chains linked by covalent bonds.

Branch-Block Copolymers Made with 1-Octene. Similar experiments were conducted to synthesize branch−block copolymers with 1-octene. The polymerization procedure was analogous to the one used for ethylene/1-butene copolymerizations. Two factors were investigated: 1-octene concentration and degree of macromonomer unsaturation. Table 12 summarizes

the conditions for these polymerization runs and Table 13 lists some polymer properties and yields.

Effect of 1-Octene Concentration. Polymerization runs L and M were done at the same macromonomer concentrations, but with different 1-octene concentrations. All other reaction conditions were the same. Two ethylene/1-octene copolymers were also made with the same 1-octene concentrations used for making samples L and M to indentify the CRYSTAF peak positions when no macromonomer was added to the reactor (samples L-O and M-O).

Figure 21 shows CRYSTAF profiles for samples L, M, L-O, M-O, and macromonomer.

Samples L and M have intermediate CRYSTAF peaks that characterize the presence of cross-product due to the incorporation of macromonomer into the growing ethylene/1-octene copolymer chains. A few interesting observations can be made regarding these CRYSTAF profiles. First, the branch−block copolymer made with the lowest 1-octene concentration (sample L) has a higher cross-product fraction, as indicated by the higher area under the intermediate CRYSTAF peak for sample L. This is in agreement with the previous observation that decreasing ethylene pressure, and thus increasing the 1-butene fraction in the copolymer, led to the production of less cross-product in the ethylene/1-butene copolymerization experiments. Second, it appears that there is a competition for insertion between 1-octene and macromonomer; the presence of macromonomer decreases the relative rate of 1-octene insertion. This is clear when comparing the positions for the L-O and M-O peaks with the lower crystallinity peaks for samples L and M, respectively. We suggest that 1-octene is less likely to be polymerized after a macromonomer insertion due to steric effects (that is, the reactivity ratio for 1-octene/macromonomer is small), effectively lowering 1-octene incorporation in the copolymer when the macromonomer concentration increases.

Figure 22 shows the MWD and log $[\eta] \times$ log M plots for samples L and M. The log $[\eta] \times$ log M curves for both samples deviate from linearity at high molecular weight, confirming the presence of long chain branching in these polymers.

If we assume that there is no interaction between macromonomer and the CGC−Ti-produced copolymer chains, we can predict the MWD of the resulting polymer by superposition of the MWDs of macromonomer and of ethylene/1-octene

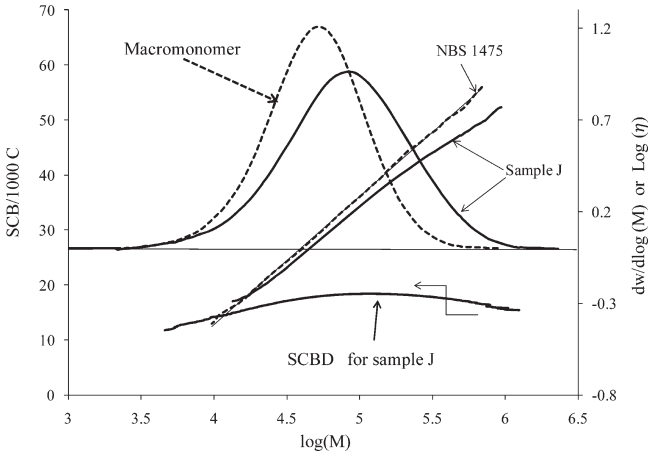

Figure 20. MWD and intrinsic viscosity plot for samples J and macromonomer.

Table 12. Polymerization Conditions for Samples L, M, L-n, and M-n[a]

sample	λ_{vinyl}	1-octene concentration (mol/L)
L	5.1	0.36
M	5.1	0.48
L-n	1	0.36
M-n	1	0.48

[a] Polymerization conditions: T = 120 °C, P = 120 psig, MM concentration = 13.5 g/L, polymerization time = 15 min, and CGC−Ti concentration = 2.44 μmol/L.

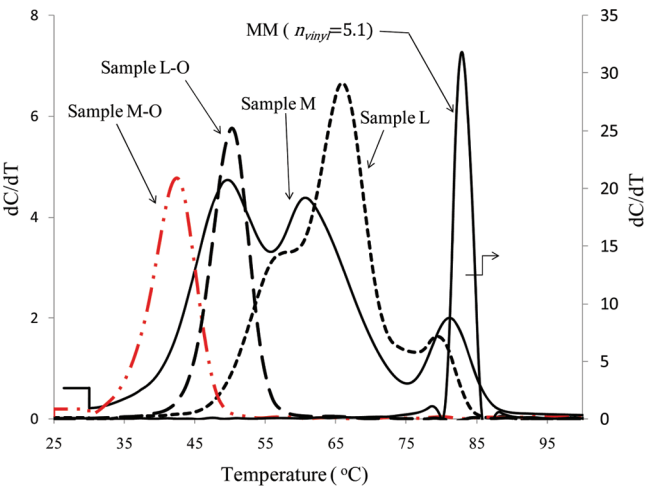

Figure 21. CRYSTAF profiles for samples M, L, M-O, L-O, and macromonomer.

Table 13. GPC Results and LCBs Calculations for Samples L, M, M-O, L-O, M-n, and L-n

	polymer mass (g)					λ_{hexyl}[a]		
sample	total	excluding MM	M_w	M_n	PDI	whole polymer	CGC−Ti polymer	n_{LCB}
MM			53 000	24 800	2.1	0	0	0.09
L	13.15	10.15	275 200	56 500	4.9	11.1	14.4	0.89
M	13.1	10.1	217 334	53 400	4.1	14.6	18.9	0.31
M-O			121 200	55 000	2.2	24	24	0
L-O			128 000	59 000	2.2	17.3	18.9	0
M-n	13.15	10.6	45 800	112 800	2.5	12.4	17.4	0
L-n	11.46	8.46	50 900	137 000	2.7	9.8	13.3	0

[a] λ_{hexyl} = average number of hexyl branches per 1000 carbon atoms.

dx.doi.org/10.1021/ma201368c |*Macromolecules* 2011, 44, 7926–7939

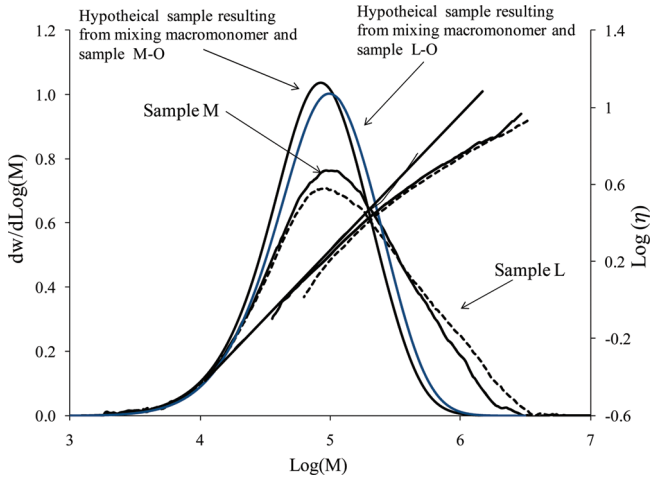

Figure 22. MWD and intrinsic viscosity plot for samples L and M.

copolymer. Figure 22 compares these hypothetical MWDs with the ones actually measured for samples L and M, clearly showing that significant chemical bonding between macromonomer and ethylene/1-octene chains took place during the polymerization.

The mass of ethylene/1-octene copolymer made in the second polymerization stage can be calculated from the initial mass of macromonomer and the final mass of branch−block copolymer. Therefore, the hexyl branch density (λ_{hexyl}, number of hexyl branches per 1000 carbon atoms) of the ethylene/1-octene copolymer made in the second stage of polymerization can be estimated using the following expression

$$m_m \times \lambda_{hexyl,m} + m_{E/O} \times \lambda_{hexyl,E/O} = m_{w\times}\lambda_{hexyl,w} \qquad (10)$$

where m_m, $m_{E/O}$, and m_w are the masses of macromonomer, ethylene/1-octene copolymer made in the second polymerization stage, and the whole polymer, respectively, and $\lambda_{hexyl,m}$, $\lambda_{hexyl,E/O}$, and $\lambda_{hexyl,w}$ are their corresponding hexyl branch density.

The hexyl branch density calculated for the ethylene/1-octene copolymer made in the second stage of polymerization for sample M is lower than the corresponding one for sample M-O, confirming that the ability of CGC−Ti to incorporate 1-octene is negatively affected by the presence of macromonomer. The same conclusion can be drawn when the hexyl branch density of ethylene/1-octene copolymers made in the second polymerization stage for samples L and L-O are compared.

The LCB frequency for sample L, calculated using the Zimm−Stockmayer approach (Table 13), is higher than that for sample M. Since the hexyl branch density for sample M (18.9 hexyl/1000 C) is higher than that for sample L (14.4 hexyl/1000 C), it can be concluded that steric hindrance of the hexyl branches might be the reason for the reduced LCB frequency in sample M.

Effect of Degree of Unsaturation in Macromonomer. It has been demonstrated above that polyethylene macromonomers having vinyl pendant double bonds resulting from ethylene/1,9-decadiene copolymerization were very effective in forming cross-product chains. To investigate whether it was possible to make similar polymers using macromonomers that contained only terminal unsaturations (no diene incorporation), two more samples (L-n and M-n) were synthesized using macromonomers produced in the absence of 1,9-decadiene. Tables 12 and 13 show

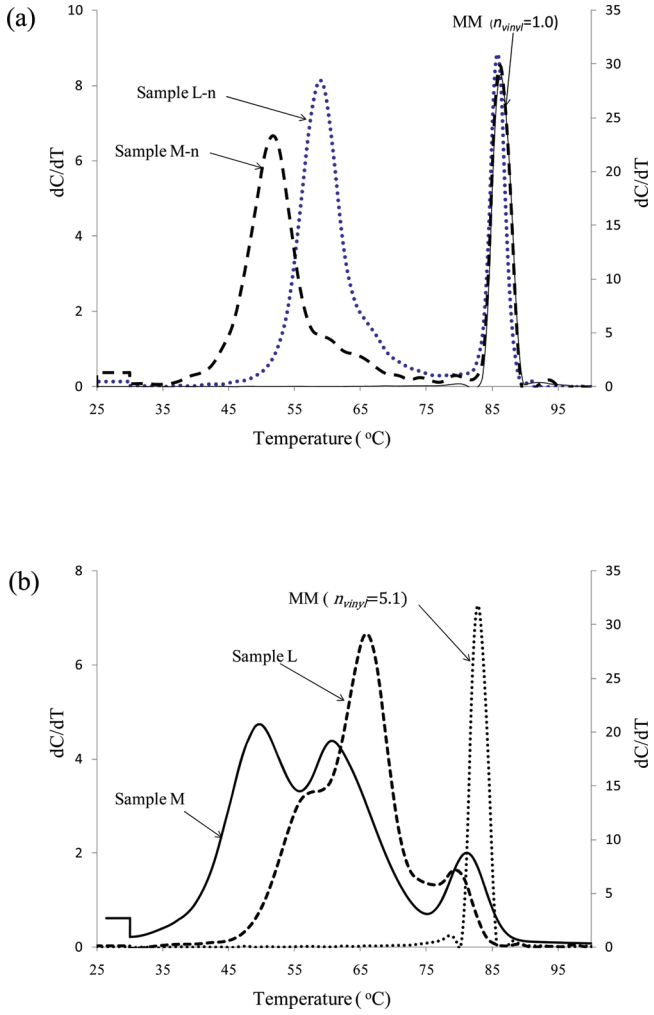

Figure 23. CRYSTAF profile for samples (a) M-n, L-n and macromonomer with $n_{vinyl=1}$ (b) samples M, L and macromonomer with $n_{vinyl=5.1}$.

polymerization conditions and properties for these polymers. Sample L-n was made under polymerization conditions similar to those used to make sample L, with the exception that the macromonomer had only terminal vinyl groups. A similar approach applies to sample M-n as compared to sample M. Figure 23 illustrates the CRYSTAF profiles of samples L, M, L-n and M-n.

The low crystallinity CRYSTAF peaks of samples L and M overlap with the corresponding low crystallinity peaks of samples L-n and M-n, respectively, since they correspond to ethylene/1-octene copolymer chains that have not reacted with the macromonomer chains.

Figure 24 shows the MWD overlaid with hexyl branch distribution for sample L-n. No LCB formation is apparent in this sample, as its log $[\eta] \times \log M$ plot is linear and overlaps the corresponding plot for the linear polyethylene NBS 1475 standard after short chain branch correction. The lack of intermediate CRYSTAF peak in Figure 23 for this sample also confirms that long chain branching is negligible. The hexyl branch density for low molecular chains is zero, increasing gradually until reaching a maximum value of 13.5 hexyl/1000C, and then remaining constant for higher molecular weight chains. This observation

dx.doi.org/10.1021/ma201368c |*Macromolecules* 2011, 44, 7926–7939

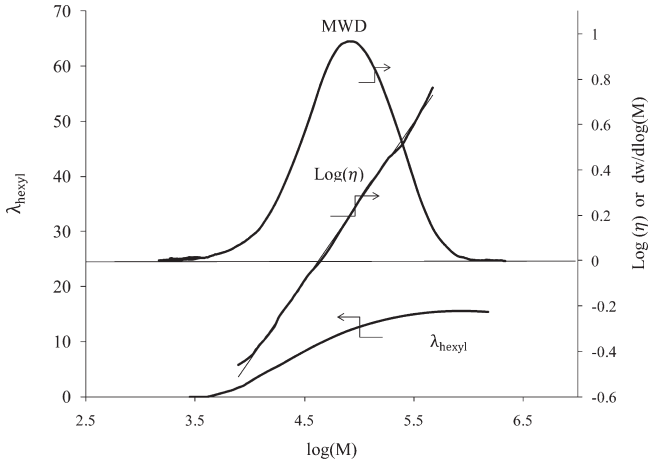

Figure 24. Molecular weight distribution, hexyl branch distribution, and viscosity plot for sample L-n.

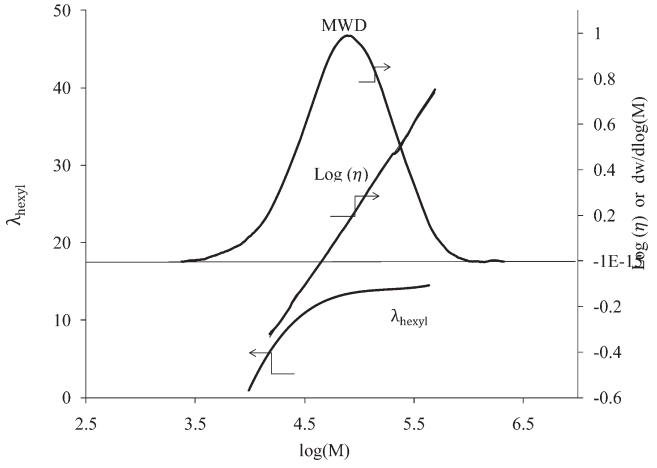

Figure 25. MWD, hexyl branch distribution, and viscosity plot for sample M-n.

indicates that macromonomer chains (with no hexyl branches) are located in the low molecular region of the MWD.

The log $[\eta] \times \log M$ plot for the sample M-n also indicate that the polymer is linear (see Figure 25) and no cross-product peak was observed in its CRYSTAF profile in Figure 23. Both observations imply that long chain branching in these polymers is below the detection range of the online GPC viscometer detector and CRYSTAF.

CONCLUSIONS

Branch−block copolymers were made in a two-stage polymerization procedure. The first stage was used to produce linear macromonomers with pendant vinyl groups. The second stage was employed to make ethylene/α-olefin/macromonomer copolymers. The proportions of the different components in the polymer (high crystallinity, low crystallinity, and cross-product) were regulated by varying reactor residence time, catalyst concentration, diene fraction, and ethylene/α-olefin ratio.

Macromonomers containing pendant 1-octenyl branches were made by copolymerizing ethylene and 1,9-decadiene using *rac*-Et(Ind)$_2$ZrCl$_2$/MAO. Increasing the diene concentration in the reactor at a constant ethylene pressure caused a linear increase in the pendant 1-octenyl branch frequency in the macromonomer, while the molecular weight-average of the polymer increased only very slightly.

Under the experimental conditions covered in this investigation, it was not possible to make branch−block copolymers with macromonomers having only terminal unsaturations, although the macromonomer made with *rac*-Et(Ind)$_2$ZrCl$_2$ had about one terminal vinyl group per chain. Introducing a small fraction of pendant vinyl groups into the macromonomer chains, however, facilitated the production of branch−block copolymer with CGC−Ti and produced a material with considerable cross-product fractions.

When macromonomers containing pendant double groups were present in the second stage of polymerization, increasing polymerization times and CGC−Ti concentration increased the weight fraction of cross-product. Increasing the ethylene pressure during the second polymerization stage at a constant 1-butene concentration produced copolymer chains with higher crystallinity and favored the formation of cross-product, likely due to steric effects associated with the sequential insertion or 1-butene and macromonomer.

When 1-octene was used as the comonomer, it was observed that an increase in 1-octene concentration decreased LCB formation, whereas an increase in pendant vinyl group frequency of the macromonomer led to increased long chain branching.

REFERENCES

(1) Soares, J. B. P.; Kim, J. D. *J. Polym. Sci., Part A: Polym. Chem.* **2000**, *38*, 1408–1416.
(2) Kim, J. D.; Soares, J. B. P.; Rempel, G. L. *J. Polym. Sci., Part A: Polym. Chem.* **1999**, *37*, 331–339.
(3) Kim, J. D.; Soares, J. B. P.; Rempel, G. L. *Macromol. Rapid Commun.* **1998**, *19*, 197–199.
(4) Kim, J. D.; Soares, J. B. P. *J. Polym. Sci., Part A: Polym. Chem.* **2000**, *38*, 1427–1432.
(5) Kim, J. D.; Soares, J. B. S. *J. Polym. Sci., Part A: Polym. Chem.* **2000**, *38*, 1417–1426.
(6) Kim, J. D.; Soares, J. B. P. *Macromol. Rapid Commun.* **1999**, *20*, 347–350.
(7) Beigzadeh, D.; Soares, J. B. P.; Duever, T. A. *Macromol. Symp.* **2001**, *173*, 179–194.
(8) Soares, J. B. P. *Macromol. Mater. Eng.* **2004**, *289*, 70–87.
(9) Sperber, O.; Kaminsky, W. *Macromolecules* **2003**, *36*, 9014–9019.
(10) Dekmezian, A. H.; Soares, J. B. P.; Jiang, P.; Garcia-Franco, C. A.; Weng, W.; Fruitwala, H.; Sun, T.; Sarzotti, D. *Macromolecules* **2002**, *35*, 9586–9594.
(11) Mehdiabadi, S.; Soares, J. B. P.; Dekmezian, A. H. *Macromol. React. Eng.* **2008**, *2*, 37–57.
(12) Arriola, D. J.; Carnaham, E. M.; Hustad, P. D.; Kuhlman, R. L.; Wenzel, T. T. *Science* **2006**, *312*, 714–719.
(13) Markel, E. J.; Weng, W.; Peacock, J.; Dekmezian, A. H. *Macromolecules* **2000**, *33*, 8541–8548.
(14) Choo, T. N.; Waymouth, R. M. *J. Am. Chem. Soc.* **2002**, *124*, 4188–4189.
(15) Pietikainen, P.; Vaananen, T.; Seppala, J. V. *Eur. Polym. J.* **1999**, *35*, 1047–1055.
(16) Pietikainen, P.; Seppala, J. V.; Ahjopalo., L.; Pietila, L. O. *Eur. Polym. J.* **2000**, *36*, 183–192.
(17) Jin, H. J.; Choi, C. H.; Park, E. S.; Lee, I. M.; Yoon, J. S. *J. Appl. Polym. Sci.* **2002**, *84*, 1048–1058.

(18) Kim, I.; Shin, Y. S.; Lee, J. K.; Cho, N. J.; Lee, J. O.; Won, M. S. *Polymer* **2001**, *42*, 9393–9403.
(19) Naga, N.; Toyota, A. *Macromol. Rapid Commun.* **2004**, *25*, 623–1627.
(20) Sarzotti, D. M.; Narayan, A.; Whitney, P. M.; Simon, L. C.; Soares, J. B. P. *Macromol. Mater. Eng.* **2005**, *290*, 584–591.
(21) Naga, N.; Imanishi, Y. *Macromol. Chem. Phys.* **2002**, *203*, 2155–2162.
(22) Mehdiabadi, S.; Soares, J. B. P.; Dekmezian, A. H. *Macromol. React. Eng.* **2008**, *2*, 529–550.
(23) Mehdiabadi, S. *Synthesis, Characterization and Polymerization Kinetics Study of Long Chain Branched Polyolefins Made with Two Single-Site Catalysts*, Ph.D. Thesis, University of Waterloo: Waterloo, Canada, 2011, p 323.
(24) Montgomery, D. C. *Applied Statistics and Probability for Engineers*, 3rd ed.; John Wiley and Sons: New York, 2003.
(25) Grant, D. M.; Paul, E. G. *J. Am. Chem. Soc.* **1964**, *86*, 2984–2986.
(26) Paul, E. G.; Grant, D. M. *J. Am. Chem. Soc.* **1963**, *85*, 1701–1702.